CoAl(001) surface structures: a kinetic Monte Carlo simulation

2009 J. Phys.: Condens. Matter 21 445005

(http://iopscience.iop.org/0953-8984/21/44/445005)

J. Phys.: Condens. Matter **21** (2009) 445005 (6pp) doi:10.1088/0953-8984/21/44/445005

CoAl(001) surface structures: a kinetic Monte Carlo simulation

Zhongjie Xu and Jun Ni

Department of Physics and Key Laboratory of Atomic and Molecular Nanoscience (Ministry of Education), Tsinghua University, Beijing 100084, People's Republic of China

E-mail: junni@mail.tsinghua.edu.cn

Received 9 April 2009, in final form 7 September 2009
Published 9 October 2009
Online at stacks.iop.org/JPhysCM/21/445005

Abstract

The growth processes of CoAl(001) films are studied by kinetic Monte Carlo simulations (KMC) combined with first principle calculations. The calculation results show that (i) for stoichiometric CoAl(001) films, the surface is occupied by pure Al; (ii) for Co slightly enriched films, the Co anti-sites segregate on the surface with a c(2 × 2) short range order; (iii) there is a peak value for the number of Co anti-sites on the surface with a change of temperature. At high temperature, the number of anti-sites c^{s}_{Co} on the surface is low because of the entropy effect. At low temperature, c^{s}_{Co} is also low because of the frozen effect. These results are in agreement with experiments, which means that the kinetic effects are important to the surface structures of CoAl(001).

(Some figures in this article are in colour only in the electronic version)

1. Introduction

The surface structures of alloys attract great interest because of their importance in technology applications. Under the effects of surface segregation, surface reconstruction, etc, the structures of alloy surfaces are usually different from the corresponding bulk structures.

The structures of TM–Al (TM = Fe, Co, Ni) surfaces have been extensively studied due to their excellent mechanical and magnetic properties. The bulk structures of TM–Al are all B2 structure [1]. However, their surface structures are different from each other. For FeAl, the (001) surface is totally Al segregated [2], while the (110) and (111) surfaces are reconstructed [3–5]. For NiAl, there are several different experimental results on the (001) surface structures [6, 7], while the (110) surface is almost bulk truncated [8, 9]. There is a tendency of Co segregation on the surface for CoAl alloys. For example, the truncated bulk structure of CoAl(110) consists of (2 × 2) atomic planes with alternating Co and Al atoms, while in the actual surface structure of CoAl(110) about 20% of Al atoms in the subsurface layer are replaced by Co atoms [10]. In the surface region of CoAl(111), the third layer under the surface is occupied by Co atoms, although Al atoms occupy this layer in the truncated bulk structure [11].

For the surface of CoAl(001), the results of first principle calculations show that the truncated bulk structure with the Al layer on the surface has lower surface energy compared to the Co surface structure and other ordered surface structures [1]. However, the results of experiments are much more complex. Blum *et al* anneal the CoAl(001) surface, which is cleaned by Ne^{+} ions under 1300 K, and find that there are Co atoms on the surface layer to form Co anti-sites. The amount is about 30% [12]. A c(2 × 2)-like short ordered structure is also found on the surface at the same temperature [12]. Under low temperature, the experiments show that there are also Co anti-sites on the surface with the concentration of about 20%. However, there are no ordered structures found on the surface [13]. One explanation [12] for the inconsistency between the first principle calculations and the experiments is as follows: the Co anti-sites on the surface are caused by the imperfect 1:1 ratio between Co and Al in the alloy. The enrichment of Co can be caused by the preference of Ne^{+} ions for Al. Based on this explanation, Wieckhorst *et al* have calculated the phase diagram of the CoAl(001) surface structures [14]. The phase diagram shows that there are several ordered structures on the CoAl(001) surface when the Co concentration is a little higher than 50%. In one of these structures, the surface layer is 4 × 4 ordered and the second layer below the surface is occupied by pure Al. In the other structure, the surface layer is 2 × 2 ordered, and the second layer below the surface is occupied by pure Co. However, the experimental results show a Co concentration of

20% in the second layer below the surface and low Co surface anti-site concentration at low temperature. The experiment of epitaxial growth of CoAl(001) films [15] also shows that at the temperature of 350 °C, with the increase of Co% from 47% to 53%, the surface structure of CoAl(001) changes from pure Al, to Al(2 × 2), then to Co(2 × 2), and finally to pure Co. These experiments at three different temperatures show that the concentration of Co anti-sites on the surface exhibits a low (20%)–high (100%)–low (30%) behavior with increase of temperature. It is meaningful to investigate the surface structures of CoAl(001) under various conditions and understand the non-monotonic relation between surface anti-site concentration and temperature.

There are various methods to deal with the film growth processes such as the rate equation [16], molecular dynamics (MD) [17] and kinetic Monte Carlo (KMC) [18] simulation. For MD and KMC studies, the interaction energies and diffusion barriers play an critical role. The cluster expansion method (CEM) [19] is widely used to determine the interaction energies. The combination of CEM and KMC has been used to simulate the growth of precipitates [20, 21], atomic clusters [22], etc. Shi *et al* simulated the growth process of Co–Pt alloy films by means of CEM and KMC, with the diffusion barriers obtained by experiments [18].

In this paper, using the CEM and KMC simulations, we have studied the growth processes of CoAl(001) films under various conditions. We find that the energy differences between Co anti-sites on the surface and in the inner layers are small, which leads to a strong entropy effect. Our results show that there is a peak in the variation of the Co anti-site concentration on the surface as a function of temperature. This non-monotonic relation between the surface Co anti-site concentration and temperature is attributed to the competition of the entropy and frozen effects. Our results are in agreement with the experiments.

In section 2 the simulation methods are described, including the Hamiltonian, the growth model of KMC, and the first principle approach. In sections 3 and 4 the simulation results are shown and discussed, including the energy parameters, the ground state, the growth processes and the surface structures under various conditions. The conclusion is given in section 5.

2. Methods

We use an lattice-gas model with pair interactions up to next nearest neighbors [18] to describe the CoAl(001) films. The Hamiltonian is written as

$$\mathcal{H} = \sum_{\{ij\}} \sum_{ss'} E^{(1)}_{ss'} \sigma^s_i \sigma^{s'}_j + \sum_{\{ij\}} \sum_{ss''} E^{(2)}_{ss''} \sigma^s_i \sigma^{s''}_j + \sum_{k\in \mathrm{surf}} \sum_{s} h_s \sigma^s_k \tag{1}$$

in which the first sum runs over all the nearest neighbors and the second sum runs over all the next nearest neighbors. Every atomic pair is counted only once. When site i is occupied by s (=Co, Al) species, $\sigma^s_i = 1$, otherwise $\sigma^s_i = 0$. If both σ^{Co}_i and σ^{Al}_i are zero, the site is occupied by a vacancy. There are therefore three states for each site: occupied by Co ($\sigma^{\mathrm{Co}}_i = 1$, $\sigma^{\mathrm{Al}}_i = 0$, $\sigma^{\mathrm{Va}}_i = 0$); occupied by Al ($\sigma^{\mathrm{Al}}_i = 1$, $\sigma^{\mathrm{Co}}_i = 0$, $\sigma^{\mathrm{Va}}_i = 0$); vacancy ($\sigma^{\mathrm{Al}}_i = \sigma^{\mathrm{Co}}_i = 0$, $\sigma^{\mathrm{Va}}_i = 1$). The interactions between atom and vacancy are considered to be zero. $E^{(1)}_{ss'}$ is the nearest neighbor interaction energy and $E^{(2)}_{ss''}$ is the next nearest neighbor interaction energy. h_s is the extra site energy of s species on the surface. This model is equivalent to a Blume–Emery–Griffiths model [23, 24].

With the Hamiltonian described above, we simulate the film growth processes by KMC simulations with the exchange model [25–27]. In our simulations, before we grow an n layer film, we first initialize an empty lattice with $n + 3$ layers. We also have used an empty lattice with $n + 6$ layers and obtained the same results. The Co and Al atoms are placed in this lattice with the method discussed below. One exchange attempt is divided into the following five steps.

(i) We check whether it is the time to grow one atom according to the growth rate. The growth rate of films is described by the parameter κ, the ratio between the rate at which the atoms are adsorbed and the atomic exchange rate. Larger κ means a faster growth process. We add one atom to the surface of the film after every $1/\kappa$ exchange attempts.

(ii) To grow one atom, we randomly choose a site that matches the growth condition, and grow a Co (Al) atom on this site with the probability equal to the concentration of Co (Al). The sites that are allowed to absorb atoms are given by the solid on solid (SOS) condition [28]. With this condition, only if all the nearest neighbors below a site are occupied, and all the nearest neighbors above the site are not occupied, is the site allowed to absorb one atom. The definition of surface is similar. The sites satisfying the SOS condition are considered to be the surface sites. Only the surface sites have the surface site energy in equation (1).

(iii) We randomly choose a site i.

(iv) We consider the vaporization process. Only if site i is a surface site and occupied by either a Co or Al atom is the atom allowed to be vaporized. The probability of vaporization is $P = \exp(-\Delta E/k_{\mathrm{B}}T)$, where $\Delta E = E_f - E_i$ is the energy difference after and before the vaporization. If the vaporization succeeds, the atom is removed from the system. Otherwise this atom remains in site i.

(v) The exchange process of the site is considered. In our simulations, only the exchanges between the nearest neighbor atom–vacancy pairs are allowed. We consider an Al atom in site i exchanging with a vacancy in the neighboring site j. $\sigma^{\mathrm{Al}}_{i(j)}$ changes from 1(0) to 0(1), $\sigma^{\mathrm{Va}}_{i(j)}$ changes from 0(1) to 1(0), while others keep unchanged. For the growth process, the diffusion on the surface is important, while in the bcc(001) lattice there are no nearest neighbors on the flat surface. So for surface sites, several other diffusion modes are allowed. One is the exchanges between an atom (vacancy) in surface site i and its next nearest neighbor vacancy (atom) in site j. Site j should also be surface site and on the same layer as site i. Another mode is the descent mode. If site i is occupied by an atom, its next nearest neighbor j is a vacancy. But site j does not satisfy the SOS condition: one or more nearest sites k of j on the layer below are vacancies. Then the atom in site i is allowed to jump to site k directly. If site k itself is not a surface site, the atom is allowed to jump to the k' site in the layer

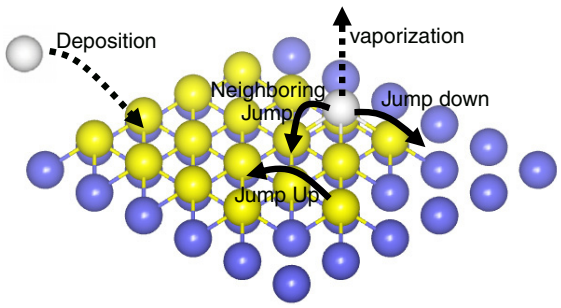

Figure 1. Schematic of surface elementary processes. The blue, yellow and white spheres stand for atoms in the first, second and third layers, respectively.

below k, until this atom jumps to a surface site. So if the final state is energetically favorable, the atom is allowed to descend more than one layer with the above diffusion mode in one exchange attempt. If site i is a vacancy, the inverse processes are also allowed as the climb-up mode. Figure 1 shows the elementary processes on the surface. For a surface site, the nearest neighbor diffusions and also the above diffusion modes are allowed; otherwise, only the nearest neighbor diffusions are allowed. The exchanges between vacancies in a surface site and its nearest neighbor in the layer below make the vacancies diffuse into the bulk. With a list of all sites that are allowed to exchange with site i, we randomly choose a site j in the list and make the exchange between site i and site j with probability $P = \exp(-U/k_BT - \Delta E/2k_BT)$ [29, 30], where U is the average exchange barrier. If $\Delta E > 2U$, the probability becomes $P = \exp(-\Delta E/k_BT)$ [30].

A Monte Carlo (MC) step means N exchange attempts, where N is the total number of sites. If the vibration frequency is ν, the real time per MC step is about N/ν. In our simulations, each layer contains 32×32 sites. The films are supposed to be grown on the substrate of Al. The initial structure is an empty lattice. In most cases, films with 20 layers are simulated.

The parameters used in KMC simulations are obtained through first principle calculations with VASP (the Vienna *ab initio* simulation package) [31]. The interaction energies in the Hamiltonian are obtained through the CEM method [19]. The calculations are performed on the eight layer Co–Al films containing 32 atoms. The atoms in the lowest four layers are kept fixed. A mesh of $9 \times 9 \times 2$ gamma centered grids is used to sample the Brillouin zone. We use the approach of Kozlowski to calculate interaction energies [32], which is similar to our previous work [33]. 16 structures are calculated in order to fit the interaction parameters. In the calculations of the barrier energies, the nudged elastic band (NEB) method is used [34, 35]. The calculations of surface barriers are performed on five layer films containing 21 atoms. The atoms in the lowest two layers are kept fixed. The $5 \times 5 \times 1$ Brillouin zone grid is used. As an approximation, we use the barrier energy of Co (Al) on a pure Co (Al) surface as the average barrier of the exchanges between next nearest neighbors on the surface [18], the climbing up and the descent down processes [36]. In the calculations of the barrier energies

Table 1. Energy parameters for the CoAl(001) surface(in eV). U is the energy barrier in the bulk and on the surface.

$E^{(1)}_{\mathrm{CoCo}}$	$E^{(1)}_{\mathrm{CoAl}}$	$E^{(1)}_{\mathrm{AlAl}}$	$E^{(2)}_{\mathrm{CoAl}}$	$h_{\mathrm{Co}} - h_{\mathrm{Al}}$
−1.7298	−1.4901	−0.8609	−0.0241	−0.9907
$U^{\mathrm{bulk}}_{\mathrm{Al-V}}$	$U^{\mathrm{bulk}}_{\mathrm{Co-V}}$	$U^{\mathrm{surf}}_{\mathrm{Al-V}}$	$U^{\mathrm{surf}}_{\mathrm{Co-V}}$	
0.48	1.42	0.63	0.68	

under the surface, we choose a $4 \times 4 \times 4$ supercell containing 127 atoms. The Brillouin zone grid is $3 \times 3 \times 3$. We only consider the barrier of Co (Al) on the bcc Co (Al). In all first principle calculations, we use the exchange–correlation functional with the generalized gradient approximation given by Perdew *et al* [37].

Since the results show no long range order in each layer, we use the short order parameters and the concentration of Co (Al), $c_{\mathrm{Co\ (Al)}}$, in each layer to describe the structures of films. The short range order parameters in the ith layer η_i are defined as $\eta_i = 1 - r_i/(c^i_{\mathrm{Co}}c^i_{\mathrm{Al}})$ [38], where r_i is the ratio between the number of Co–Al next nearest neighbor atom pairs and the total number of atom (vacancy) pairs in the ith layer. $\eta_i = 1$ indicates a totally phase separated (1×1) structure, while $\eta_i = -1$ indicates a perfect c(2×2) order structure. For a random structure, $\eta_i = 0$.

3. The energy parameters

The CEM results for the interaction energies between Co and Al and the energy barriers are shown in table 1. These energy parameters are used to simulate the structures of CoAl, no new stable structure different from the above 16 kinds of structures, which we used to fit the energy parameters, are obtained using Monte Carlo simulations. Although the site energy of Co atoms on the surface is about 1 eV lower than that of Al atoms, the stoichiometric CoAl(001) film is Al segregated because of the large energy difference between $E^{(1)}_{\mathrm{CoAl}}$ and $E^{(1)}_{\mathrm{AlAl}}$. For the non-stoichiometric CoAl(001) film, there are Co anti-sites in the Al layers. Since there are few Al anti-sites in Co layers, we can approximately estimate the energy difference between one Co anti-site on the surface and one in the inner layer by considering the case where there are no Al anti-sites in Co layers. Then one Co anti-site on the surface and one Al atom in the bulk have the energy of

$$E_1 = 4E^{(1)}_{\mathrm{CoCo}} + h_{\mathrm{Co}} + 8E^{(1)}_{\mathrm{CoAl}} + E^{(2)}_{\mathrm{CoAl}}(4 + n^{\mathrm{s}} - n^{\mathrm{i}}) \quad (2)$$

while one Co anti-site in the bulk and one Al atom on the surface have the energy of

$$E_2 = 4E^{(1)}_{\mathrm{CoAl}} + h_{\mathrm{Al}} + 8E^{(1)}_{\mathrm{CoCo}} + E^{(2)}_{\mathrm{CoAl}}(4 - n^{\mathrm{s}} + n^{\mathrm{i}}) \quad (3)$$

where $n^{\mathrm{s\ (i)}}$ is the number of the nearest neighbor Al atoms on the surface (inner layers). Thus the energy difference between one Co anti-site on the surface and one in the inner layers is $\Delta E = -0.0412 - 0.0481 \times (n^{\mathrm{s}} - n^{\mathrm{i}})$ (eV). The first item comes from both the site energy and the nearest neighbor interaction energy. The second item comes from the second

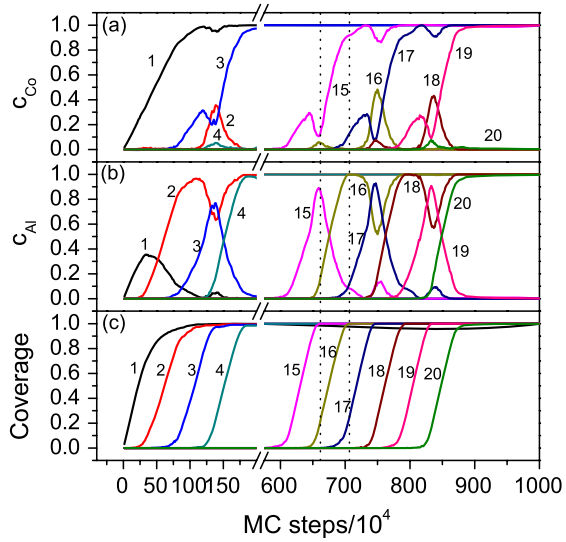

Figure 2. The growth processes of the stoichiometric CoAl(001) films with 20 layers at $T = 1300$ K and $\kappa = 10^{-7}$. (a) The time evolution of Co concentration. (b) The time evolution of Al concentration. (c) The time evolution of coverage. The labels 1–20 indicate the sequence number of layers. 20 corresponds to the surface layer. The perpendicular dotted lines show the time at which the coverages of layers 15 (odd) and 16 (even) reach unity.

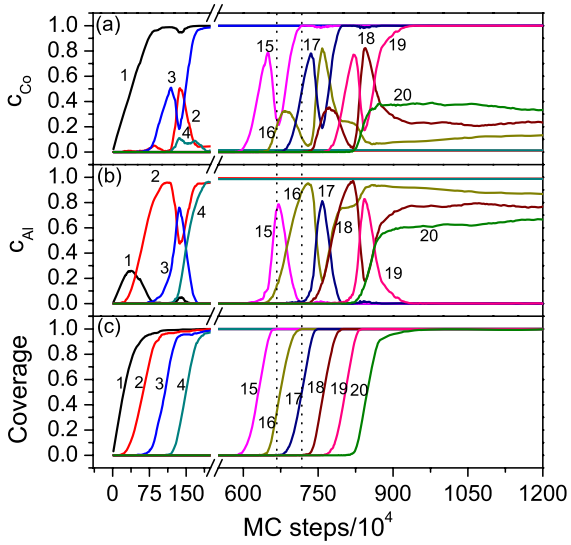

Figure 3. The growth processes of 20 layer CoAl(001) films with the Co concentration of 55% at $T = 1300$ K and $\kappa = 10^{-7}$. (a) The time evolution of Co concentration. (b) The time evolution of Al concentration. (c) The time evolution of coverage. The labels 1–20 indicate the sequence number of layers. 20 corresponds to the surface layer. The perpendicular dotted lines show the time at which the coverages of layers 15 (odd) and 16 (even) reach unity.

nearest neighbor interaction energy. The nearest interaction is not dominant and the value of E is comparable to k_BT at high temperature, which means that the effect of entropy is important for the surface structures of CoAl(001).

4. The surface structures

We have calculated the growth process of the CoAl(001) films with 20 layers. First we discuss the results of the stoichiometric CoAl(001) films. The time evolution of the Co and Al concentrations and the total coverage in each layer of the films are shown in figure 2. The results show that for the stoichiometric CoAl(001) films there are no Co atoms on the surface, which is consistent with the results of first principle calculations [1]. The time evolution of the total coverage shows that at the temperature of 1300 K the growth processes of all the odd (even) layers except the surface are similar. When the coverage of an odd layer reaches unity, there are about 80% Al and 20% Co on this layer. The calculations show that about 30% sites of the upper layer are occupied, most of which are occupied by Al. This phenomenon indicates that there is an Al segregation on the CoAl(001) surface. When the coverage of an even layer reaches unity, the layer is occupied by pure Al, with about 25% of the sites of the upper layer occupied by equal numbers of Al and Co. These Co atoms do not tend to jump to the Al layer under the surface. The growth process of films with 55% Co is shown in figure 3, which is different from the stoichiometric 50% Co case shown in figure 2. When the coverage of either an even or odd layer reaches unity, there are about 20% Co atoms in the layer, with most covered sites occupied by Co atoms in the upper layer. Figure 4 is a schematic picture showing the profile structures of CoAl films when the coverage of an even layer reaches unity. This phenomenon could be regarded as the segregation of Co anti-sites on the surface. After the growth finishes, a number of Co anti-sites appear on the surface and the second layer below the surface, with the Co concentrations of 27.0% and 23.8% respectively. There are Co anti-sites in other even layers, but the concentrations are much lower. All these differences are due to the effect of the much lower surface energy of Co. Rather than evenly distributing in the bulk, the Co anti-sites prefer to segregate on the surface region. The calculated concentrations of Co anti-sites on the surface and the second layer below the surface are close to the experimental results [12] of 30% and 20%, respectively. The surface of the films is partially ordered, which is different from the perfectly c(2 × 2) ordered structure in [14]. The short range order parameter of the surface layer is −0.4, in good agreement with the experimental value of −0.4 for the best fit structure of LEED data in [12].

The surface concentrations c^s_{Co} as a function of the total Co concentrations for 20 layer films at the temperature of 1300 K are shown in figure 5. All data in figures 5–7 are averaged over 20 repetitions. At low concentration, since the total number of Co atoms is not large enough, most Co anti-sites gather in the surface region. The Co concentrations c_{Co} of the surface and the second layer below the surface are 0.148 and 0.108 respectively, while c_{Co} of other layers are less than 3%. With the increase of Co concentration, more Co anti-sites gather on the surface layer. The increase of c^s_{Co} is almost linear at first. At high concentration, c^s_{Co} exhibits a plateau at the value of about 37%, which indicates that the increase of the total Co concentration has little contribution to the anti-sites on the surface layer at concentration higher than 64%.

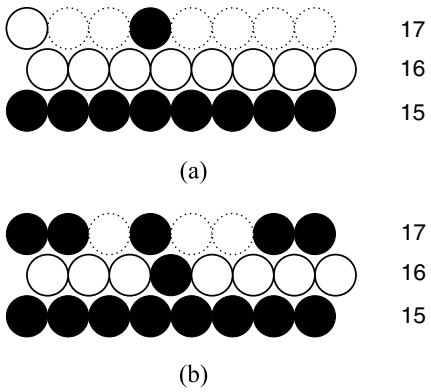

Figure 4. The schematic profile structures of films with (a) 50% Co and (b) 55% Co when the coverage of layer 16 reaches unity. The black, white and dashed circles are Co, Al and empty site, respectively. Labels 15–17 indicate the number of layers.

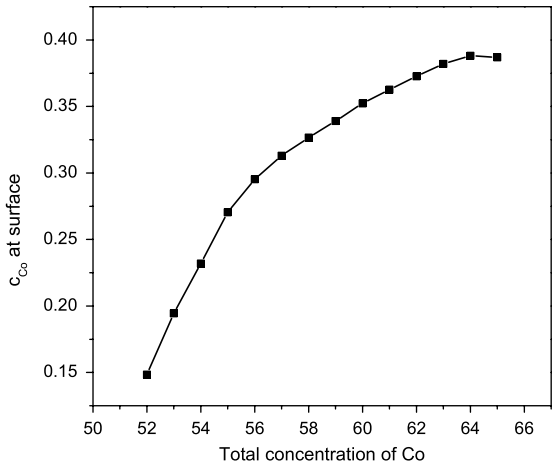

Figure 5. The Co surface concentration c^{s}_{Co} of the films with 20 layers as a function of the total Co concentration with $T = 1300$ K and $\kappa = 10^{-7}$. The data are averaged over 20 repetitions.

We have also calculated the growth processes of films with different layers at the Co concentration of 55% and the temperature of 1300 K. The time evolutions of the Co and Al concentrations are similar to those for the 20 layer films. The c_{Co} in the even layers are shown in figure 6. Films with different layers have similar c_{Co} in the first several even layers near the surface and near the substrate, which means that, although there are more Co anti-sites in the films with more layers, the c_{Co} near the surface keep unchanged. The c_{Co} gradient near the surface does not change with the film thickness. For thicker films, the surplus anti-sites are almost evenly distributed in the inner layers. To compare with the ground state of the films, we have done an energy minimization of the films with the Co concentration of 55%, assuming that there are no Al anti-sites in Co layers. The results show that there are 50% Co anti-sites on the surface, forming a perfect c(2 × 2) structure, which is similar to one of the structures in [14], and there are no Co anti-sites in the inner layers. The ground state structure is different from the above results of KMC simulations at the temperature of 1300 K. We attribute

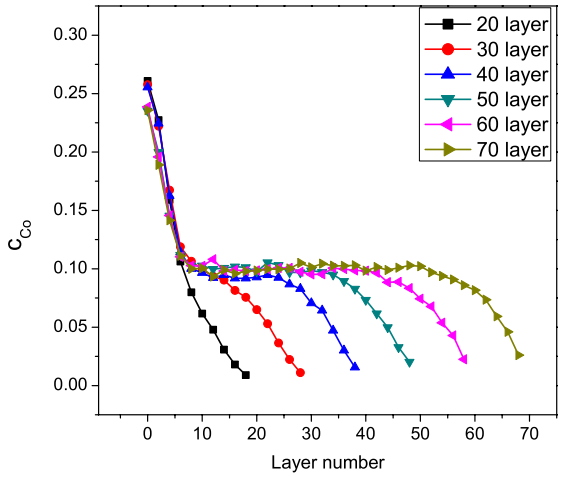

Figure 6. Co concentrations c_{Co} in the even layers as a function of layer number with the total Co concentration of 55%, $T = 1300$ K and $\kappa = 10^{-7}$. For a clear comparison, the layer number of the surfaces is counted as 0. The data are averaged over 20 repetitions.

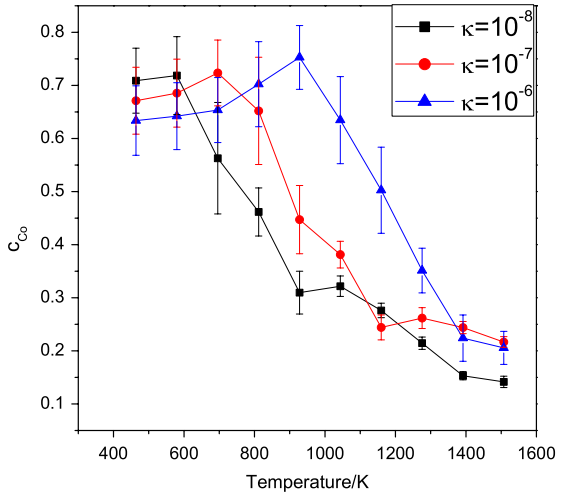

Figure 7. Surface Co concentration c^{s}_{Co} as a function of temperature under different deposition rates. The total Co concentration is 55%. The data are averaged over 20 repetitions.

this difference to the effect of entropy. Since the energy difference of Co anti-sites on the surface and in the inner layers is small, the entropy plays an important role in the free energy difference at high temperature, which results in a much lower c^{s}_{Co} than the ground state and a nonzero Co concentration in the second layer below the surface.

Figure 7 shows the relation between c^{s}_{Co} and temperature with different deposition rates. It should be noted that the change with the temperature is not monotonic. There is a peak in the curve for $\kappa = 10^{-6}$, which means that the c^{s}_{Co} have the maximum values at medium temperature. This explains the similar experimental phenomena. As mentioned above, at high temperature, the effect of entropy reduces the Co anti-sites on the surface. When the temperature decreases, the entropy effect becomes smaller, resulting in the increases of c^{s}_{Co}. On the other hand, when the temperature is lower, the frozen effect becomes more important [39]. At low temperature, Co

atoms do not have enough time to exchange on the surface before new atoms have covered them. For these Co atoms in the inner layers, since the exchange barrier in the bulk is very large, it is almost impossible for them to segregate on the surface layer. They are frozen in the inner layers. As a result, there are fewer Co anti-sites in the surface region compared to the situation at higher temperature. The entropy effect and frozen effect compete, which determines the value of c^{s}_{Co}. For smaller κ, there are also possible peaks in the curves. The temperature T_{max} for the maximum c^{s}_{Co} increases with the increase of growth rate as shown in figure 7. The reason is that, with the decrease of growth rate, there is more time for the Co anti-sites to segregate on the surface layer, which reduces the frozen effect and makes T_{max} lower. The relation between c^{s}_{Co} and temperature is in agreement with the low–high–low behavior exhibited in experiments [12, 13, 15], which means that the surface structure of CoAl(001) is affected by kinetics. The underlying mechanism may also be effective for other alloys where the energy differences between anti-sites on the surface and in the bulk are small.

5. Conclusions

We have performed KMC simulations for CoAl(001) films with various compositions. The results show that for the stoichiometric CoAl(001) films the surface is occupied by pure Al, while for Co rich CoAl(001) films the Co anti-sites segregate on the surface, forming a c(2 × 2) short range ordered surface. We find that the energy difference between one Co anti-site on the surface and one in the inner layers, which is determined by the formula $\Delta E = -0.0412 - 0.0481 \times (n^{s} - n^{i})$, is small and thus the effect of entropy is important. At high temperature, the effect of entropy makes c^{s}_{Co} smaller than its ground state value. With the decrease of temperature, the surface Co concentration c^{s}_{Co} increases because the entropy effect becomes weaker. At low temperature, the frozen effect becomes more important, which prevents Co atoms in the bulk from segregating on the surface. As a result, for $\kappa = 10^{-6}$, there is a peak temperature T_{max} below which c^{s}_{Co} begins to decrease with the decrease of temperature due to the more prominent frozen effect. For $\kappa = 10^{-7}, 10^{-8}$, there are also possible peaks. The peak temperature T_{max} becomes lower with the decrease of deposition rate. The low–high–low behavior of c^{s}_{Co} with the increase of temperature is in qualitative agreement with experiments, which means that the kinetic effects are important to the surface structures of CoAl(001).

Acknowledgments

This research is supported by the National Natural Science Foundation of China (Nos 10674076 and 10721404) and MOST (2006CB605105).

References

[1] Müller S 2003 *J. Phys.: Condens. Matter* **15** R1429
[2] Wang C P, Jona F, Gleason N R, Strongin D R and Marcus P M 1993 *Surf. Sci.* **298** 114
[3] Hammer L, Graupner H, Blum V, Heinz K, Ownby G W and Zehner D M 1998 *Surf. Sci.* **412+413** 69
[4] Baddorf A P and Chandavarkar S S 1996 *Physica* B **221** 141
[5] Kizilkaya O, Hite D A, Zehner D M and Sprunger P T 2004 *J. Phys.: Condens. Matter* **16** 5395
[6] Blum R P, Ahlbehrendt D and Niehus H 1996 *Surf. Sci.* **366** 107
[7] Stierle A, Formoso V, Comin F and Franchy R 2000 *Surf. Sci.* **467** 85
[8] Davis H L and Noonan J R 1985 *Phys. Rev. Lett.* **54** 566
[9] Hanbicki A T, Baddorf A P, Plummer E W, Hammer B and Scheffler M 1995 *Surf. Sci.* **331–333** 811
[10] Daw M S and Baskes M I 1983 *Phys. Rev. Lett.* **50** 1285
[11] Hammer L, Blum V, Schmidt Ch, Wieckhorst O, Meier W, Müller S and Heinz K 2005 *Phys. Rev.* B **71** 075413
[12] Blum V, Hammer L, Schmidt Ch, Meier W, Wieckhorst O, Müller S and Heinz K 2002 *Phys. Rev. Lett.* **89** 266102
[13] Rose V, Brüggemann K, David R and Franchy R 2007 *Phys. Rev. Lett.* **98** 037202
[14] Wieckhorst O, Müller S, Hammer L and Heinz K 2004 *Phys. Rev. Lett.* **92** 195503
[15] Maeda N, Kawashima M and Horikoshi Y 1995 *J. Appl. Phys.* **78** 6013
[16] Colayni G and Venkat R 2000 *J. Cryst. Growth* **211** 21
[17] Miron R A and Fichthorn K 2004 *Phys. Rev. Lett.* **93** 138201
[18] Shi L and Ni J 2006 *Phys. Rev. Lett.* **97** 126105
[19] Ozolins V, Wolverton C and Zunger A 1998 *Phys. Rev.* B **57** 6427
[20] Mueller S, Wang L-W and Zunger A 2002 *Modelling Simul. Mater. Sci. Eng.* **10** 131
[21] Slabanja M and Wahnström G 2005 *Acta Mater.* **53** 3721
[22] Chepulskii R V and Butler W H 2005 *Phys. Rev.* B **72** 134205
[23] Blume M, Emery V J and Griffiths R B 1971 *Phys. Rev.* A **4** 1071
[24] Ni J and Iwata S 1995 *Phys. Rev.* B **52** 3214
[25] Binder K and Heermann D W 1988 *Monte Carlo Simulation in Statistical Physics: an Introduction* (Berlin: Springer)
[26] Kawasaki K 1966 *Phys. Rev.* **145** 224
[27] Venables J A, Spiller G D T and Hanbücken M 1984 *Rep. Prog. Phys.* **47** 399
[28] Gilmer G H and Bennema P 1972 *J. Appl. Phys.* **43** 1347
[29] Vineyard G H 1956 *Phys. Rev.* **102** 981
[30] Xu Z J, Hao Z H, Ni J and Iwata S 2009 *Thin Solid Films* **517** 1848
[31] Kresse G and Hafner J 1993 *Phys. Rev.* B **47** R558
Kresse G and Hafner J 1994 *Phys. Rev.* B **49** 14251
Kresse G and Furthmüller J 1996 *Phys. Rev.* B **54** 11169
[32] Kozlowski M, Kozubski R, Pierron-Bohnes V and Pfeiler W 2005 *Comput. Mater. Sci.* **33** 287
[33] Shi L and Ni J 2008 *Phys. Rev.* B **77** 035407
[34] Henkelman G, Uberuaga B P and Jónsson H 2000 *J. Chem. Phys.* **113** 9901
[35] Henkelman G and Jónsson H 2000 *J. Chem. Phys.* **113** 9978
[36] Han Y, Unal B, Qin F, Jing D, Jenks C J, Liu D, Thiel P A and Evans J W 2008 *Phys. Rev. Lett.* **100** 116105
[37] Perdew J P, Chevary J A, Vosko S H, Jackson K A, Pederson M R, Singh D J and Fiolhais C 1992 *Phys. Rev.* B **46** 6671
[38] Cowley J M 1950 *Phys. Rev.* **77** 669
[39] Shi L and Ni J 2004 *Phys. Rev.* B **69** 155428